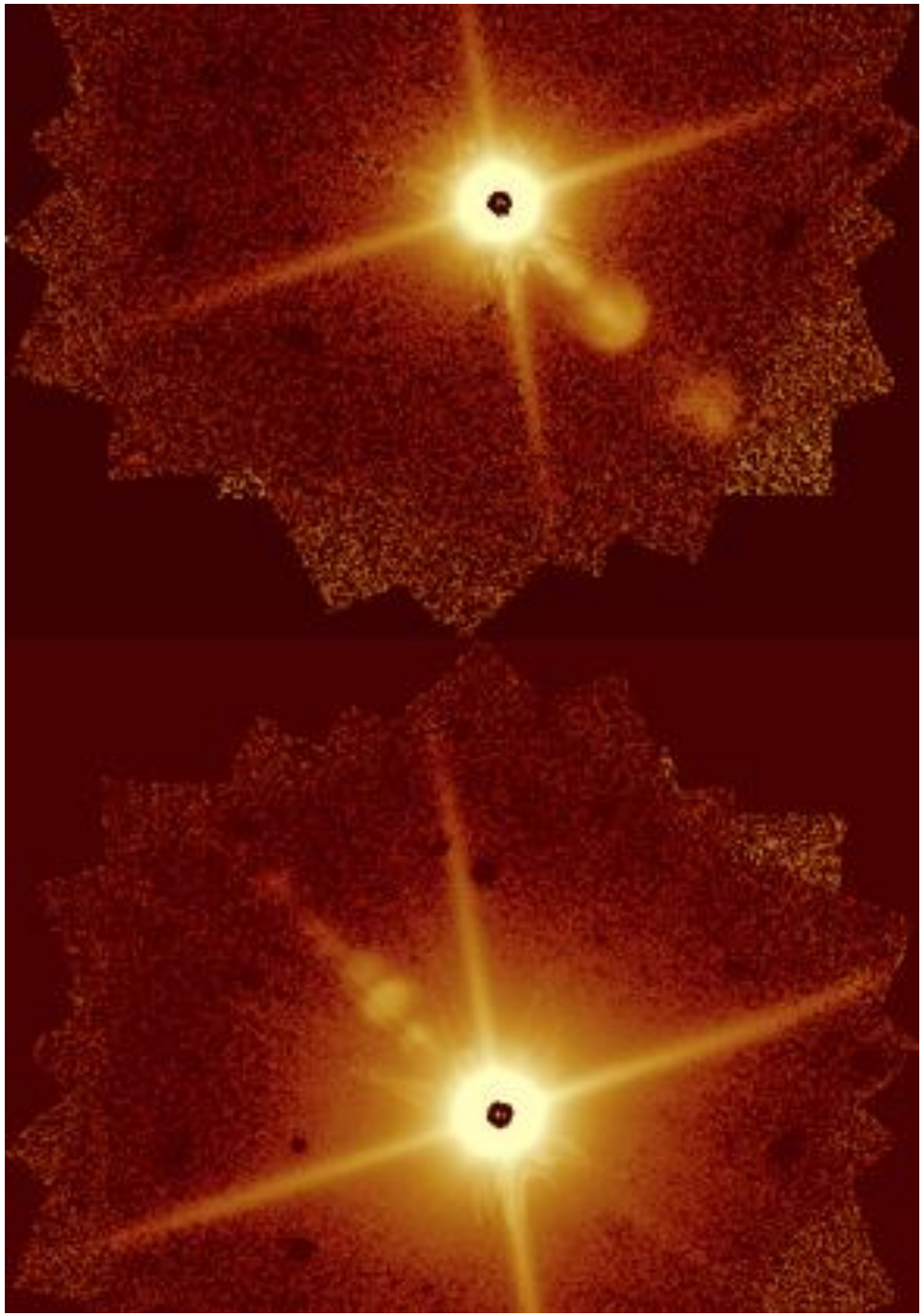

Maynooth University
National University of Ireland Maynooth

Jets from YSOs: The MUSE Perspective

Aisling Murphy
Maynooth University, Department of Experimental Physics

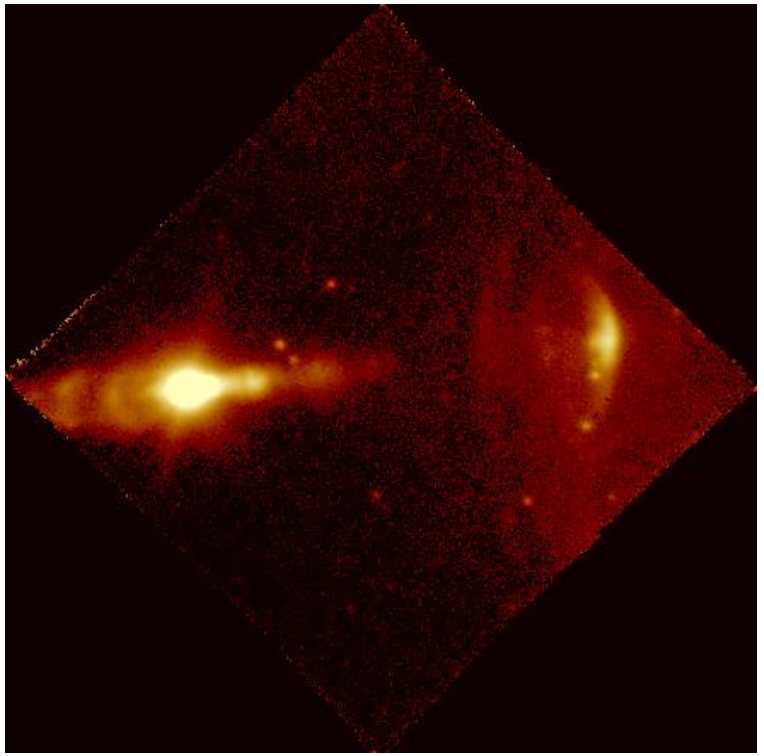

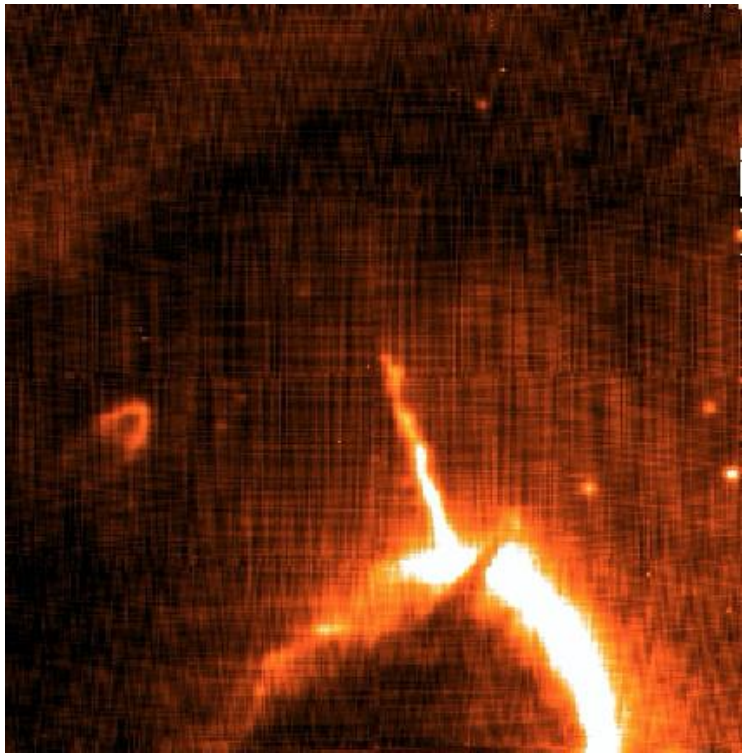

Maynooth University
National University of Ireland Maynooth

Collaborators

Emma Whelan, Maynooth University, PhD supervisor

Catherine Dougados
Francesca Bacciotti
Deirdre Coffey
Christian Schneider
Fernando Comerón
Juan Alcalá
Tom Ray
Paulo Garcia
Jochen Eislöffel
Brunella Nisini

Maynooth University
National University of Ireland Maynooth

Integral Field Spectroscopy

- Rapid collection of spatial and spectral data
- IFS suffers significantly less from spurious effects introduced by the use of adaptive optics, making it especially compatible with this technique
- Enables us to study the morphology, conditions and kinematics of the jet at the same time - very important for building diagnostic maps
- Typically a trade-off between spatial and spectral coverage

IFS and Jets

Agra-Amboage et al (2011) – used SINFONI (NIR) to analyse DG Tau jet in Fe lines including structure, kinematics and mass-flux densities

- 11000-245000 angstroms in separate H and K bands
- Max FOV 8”x8”
- R ~2000-4000

Lavalley-Fouquet et al (2000) – Used OASIS to investigate physical conditions and heating mechanisms in DG Tau

- 6200-6550 and 6500-6850 Angstrom bands (optical) – covers key emission lines for diagnostics
- FOV 5”x6.2”
- R ~ 3000-4000

Beck et al (2006) – Used GMOS on Gemini to investigate electron density in HH34

- 6220-6840 Angstrom spectra (contamination due to slit overlap)
- FOV 7”x5” (repeated for 3 separate pointings over four nights)

- Most IFS instruments designed for NIR to take advantage of adaptive optics.
- Relatively large wavelength coverage in this region but not simultaneously.
- Small fields of view

Maynooth University
National University of Ireland Maynooth

Spectroscopy with MUSE

Multi-Unit Spectroscopic Explorer (MUSE)

- Second-generation instrument on the VLT (2014)
- Integral Field Spectroscopy (IFS) optical-NIR instrument (4000-9000 Å) with medium spectral resolution.
- Good angular resolution across a 1'x1' field of view.
- GALACSI AO system adds narrow-field mode with 0.025" pixel sampling over a 7.5"x7.5" field of view
- MUSE enables simultaneous acquisition of high-resolution images and spectra, important when observing highly variable CTTS sources.
- Very broad spectral range in single exposure.

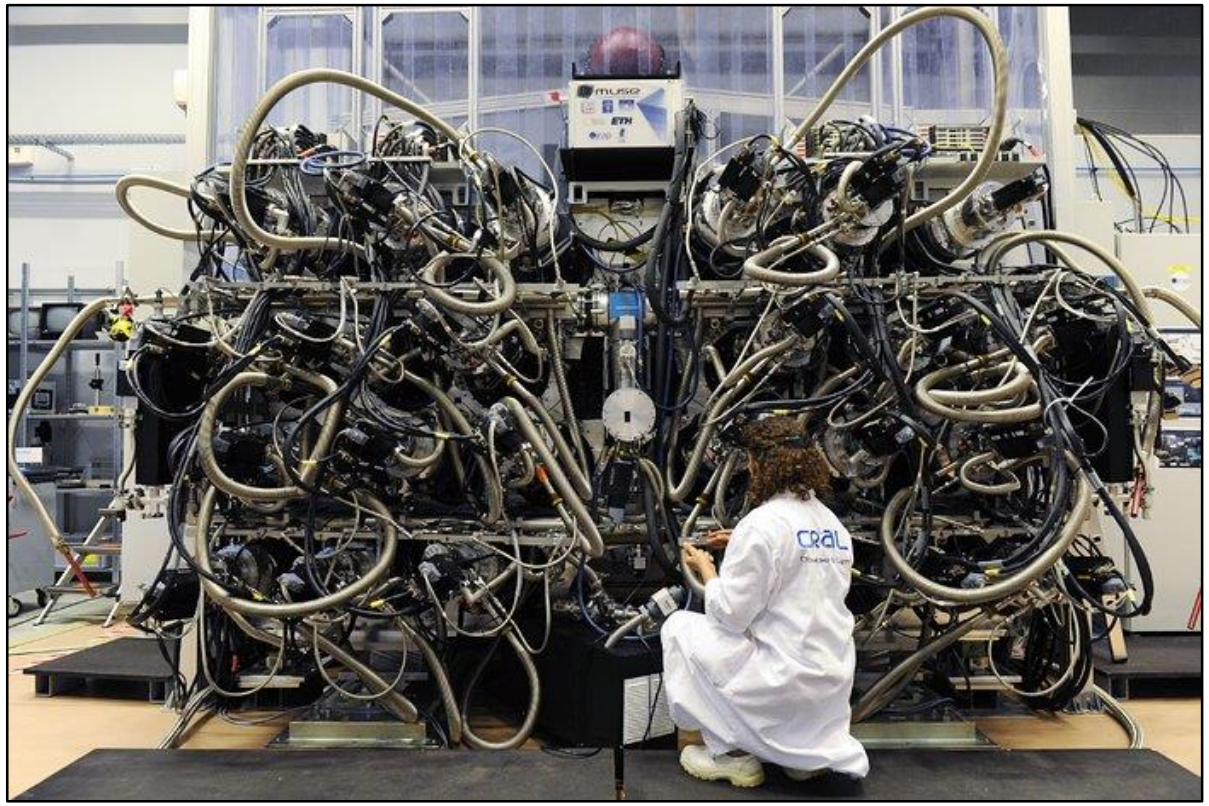

Th28 (Sz 102)

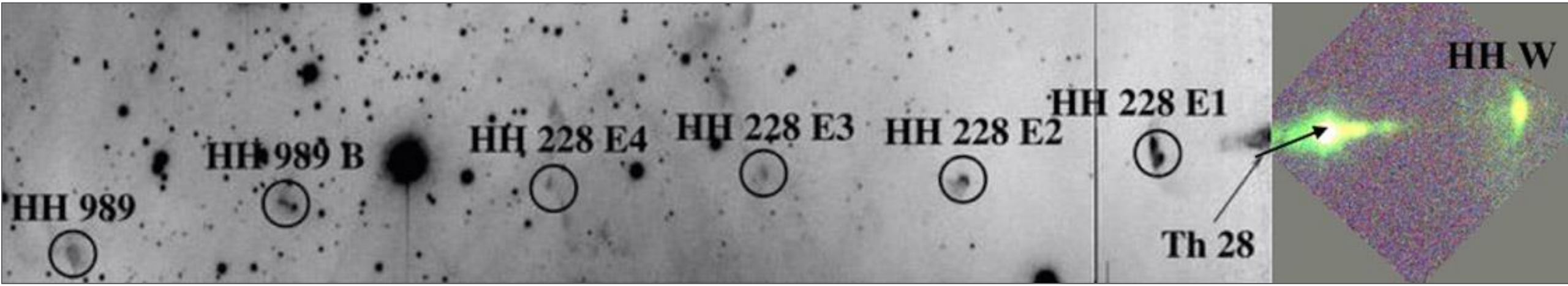

- 1-2 solar mass CTTS in the Lupus 3 cloud
- Possesses a bipolar jet (previously estimated at 0.32pc in length) that is well-resolved in optical and infrared studies.
- Herbig-Haro objects along the jet axis - knots of denser shock-excited nebula material

Maynooth University
National University of Ireland Maynooth

Th28 With MUSE

- The MUSE observations were made on 23rd June 2014. The average seeing was 0.”9 during the observations. The observations were taken so that the long axis was aligned with the jet PA and so that the red-shifted jet was mostly within the frame.

- Total integration time was 600s. The pixel scale was 0”.2. The data was reduced using the latest version of the ESO MUSE pipeline.

- Wavelength-dependent spectral resolution of between 170 km s^{-1} (4750 Å) and 75 km s^{-1} (9350 Å).

- Linear baseline subtraction used to remove stellar continuum and background stars

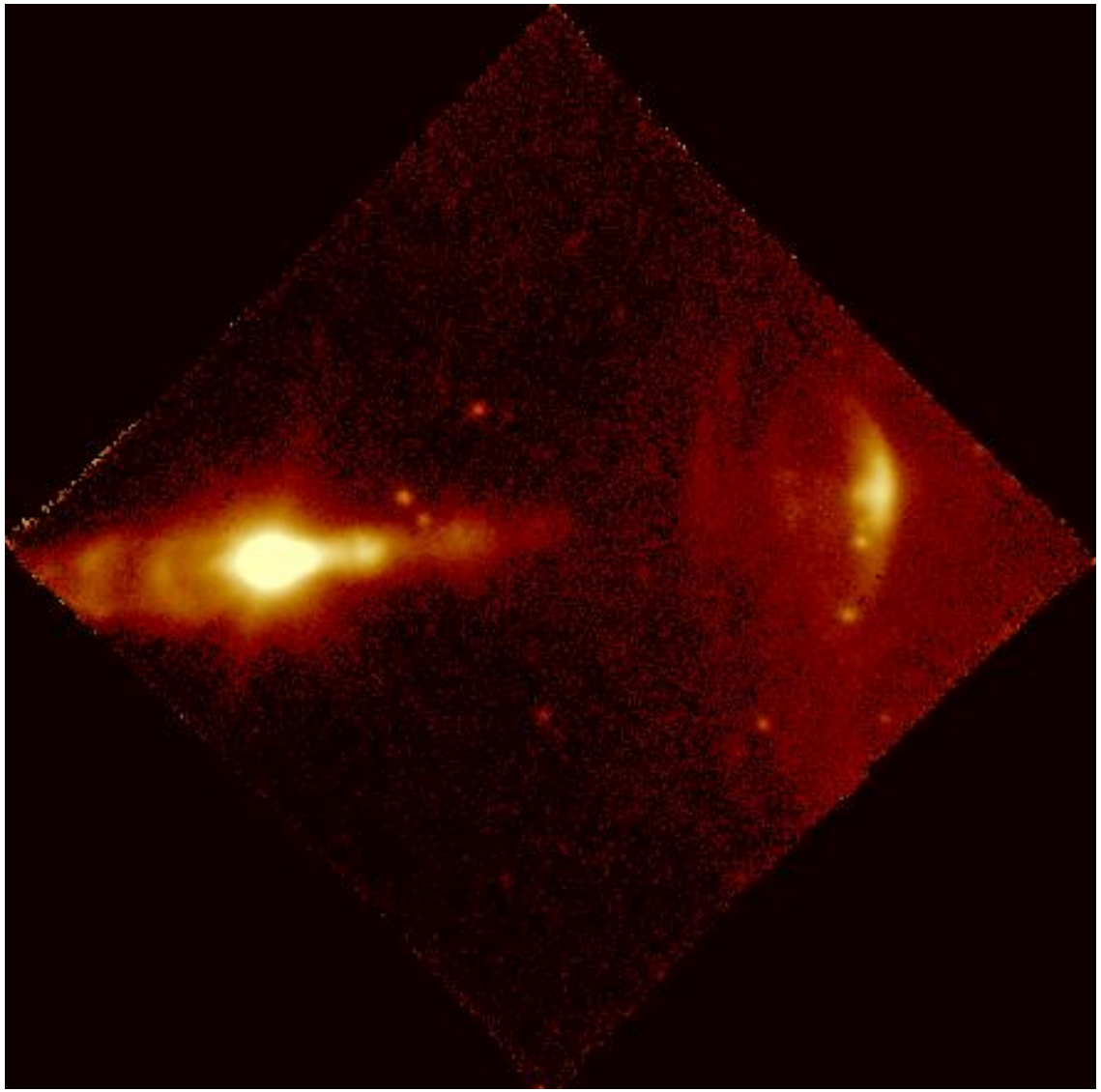

Maynooth University
National University of Ireland Maynooth

Deconvolution (OI 6300 Line)

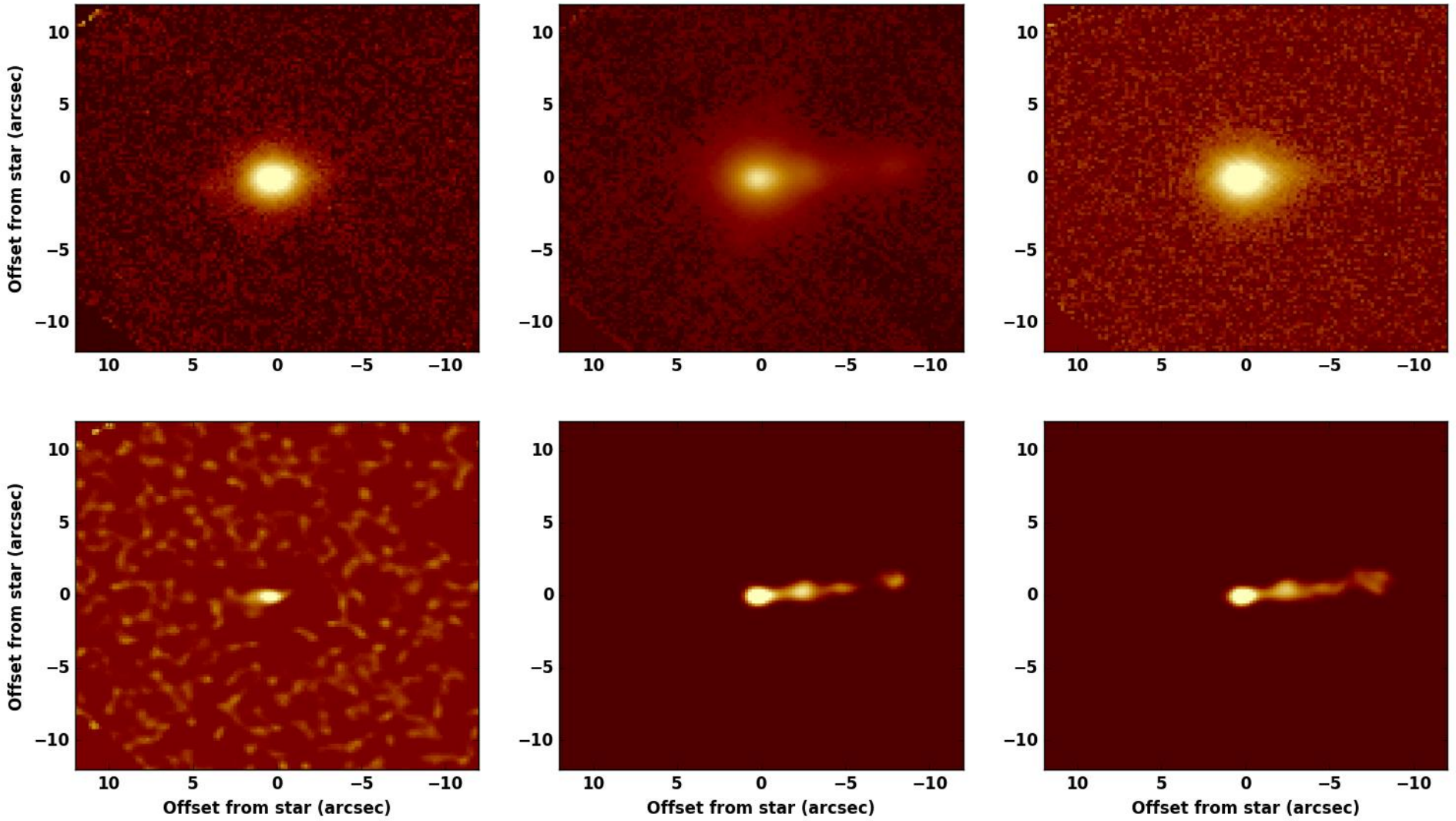

Blueshifted emission **Central velocity bin** **Redshifted emission**

Maynooth University
National University of Ireland Maynooth

PV – Diagrams

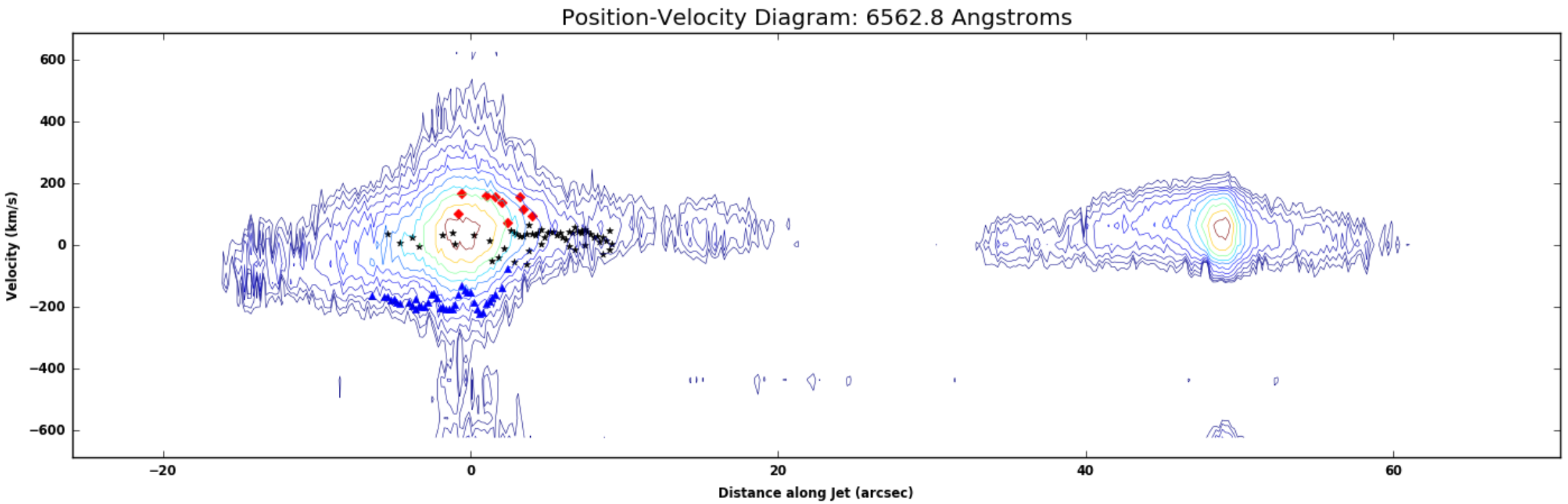

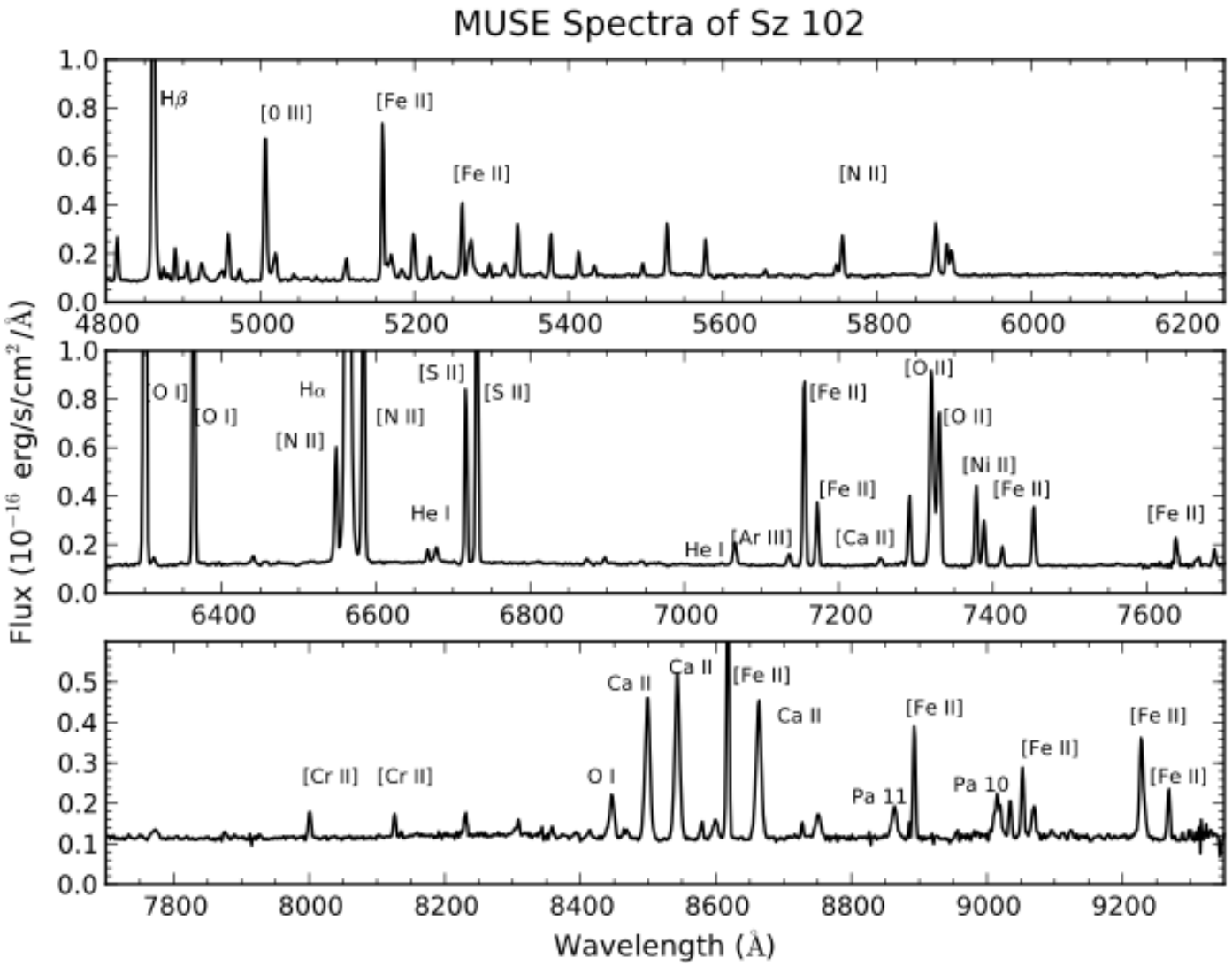

- Numerous accretion and jet tracing lines present in the spectrum of Th28
- Forbidden emission lines in the redshifted jet used to investigate physical conditions using diagnostic code based on the Bacciotti-Eislöffel method (Bacciotti & Eislöffel, 1999)

Maynooth University
National University of Ireland Maynooth

Early Diagnostic Results with MUSE

n_e (cm^{-3})

(Log scale)

n_H (cm^{-3})

(Log scale)

T_e (K)

(Log scale)

x_e

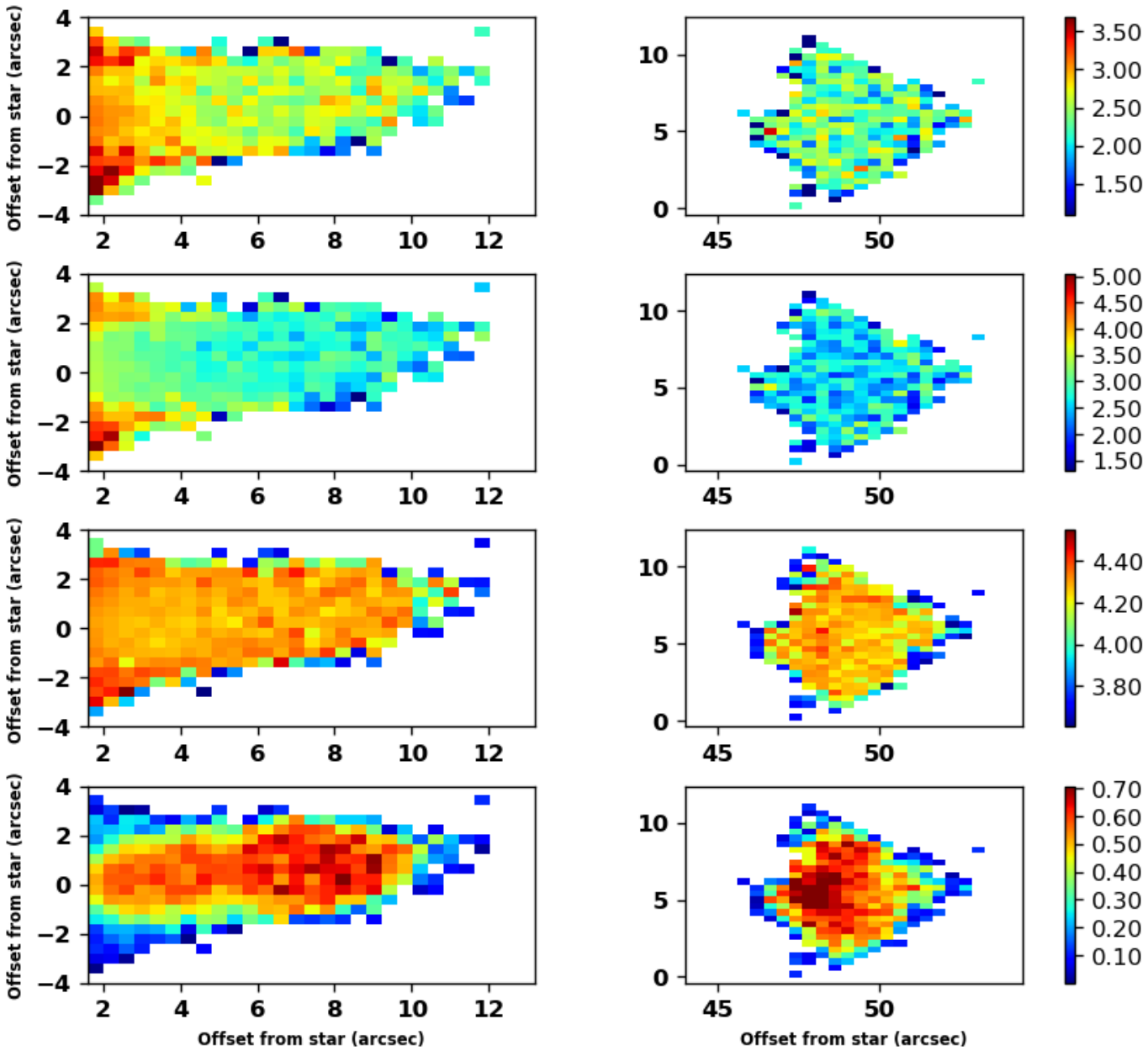

Maynooth University
National University of Ireland Maynooth

Complementing MUSE with X-Shooter

- Make use of 2015 X-Shooter observations to provide data from broadband spectroscopy.
- X-Shooter is a second-generation VLT instrument: a long-slit spectrograph with medium resolution in the UV-NIR range (3000 – 25000 angstroms).
- NIR data in particular allows broader range of diagnostic lines to be used and offers complementary estimates of mass loss rate from FeII lines
- Accretion rate difficult to determine due to lack of information on stellar mass, however the accretion luminosity can be determined using line fluxes

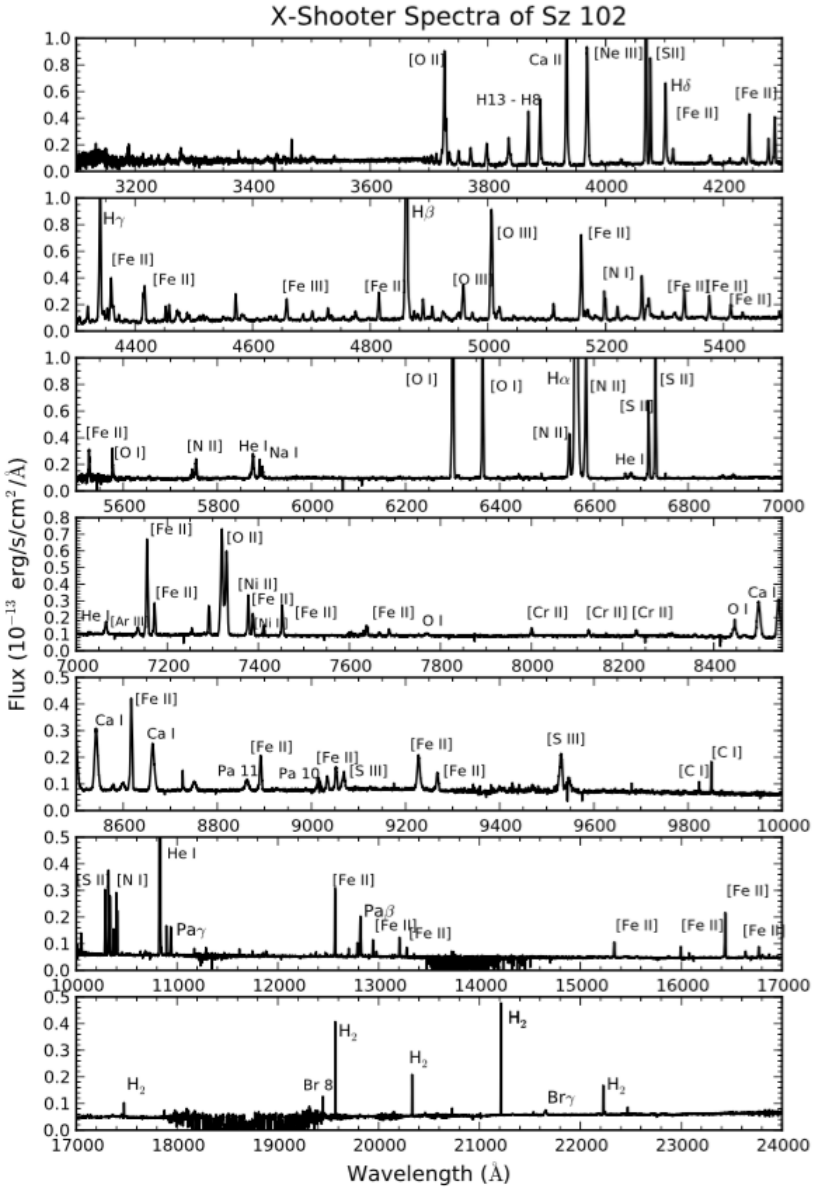

HH 399 – An Irradiated Jet

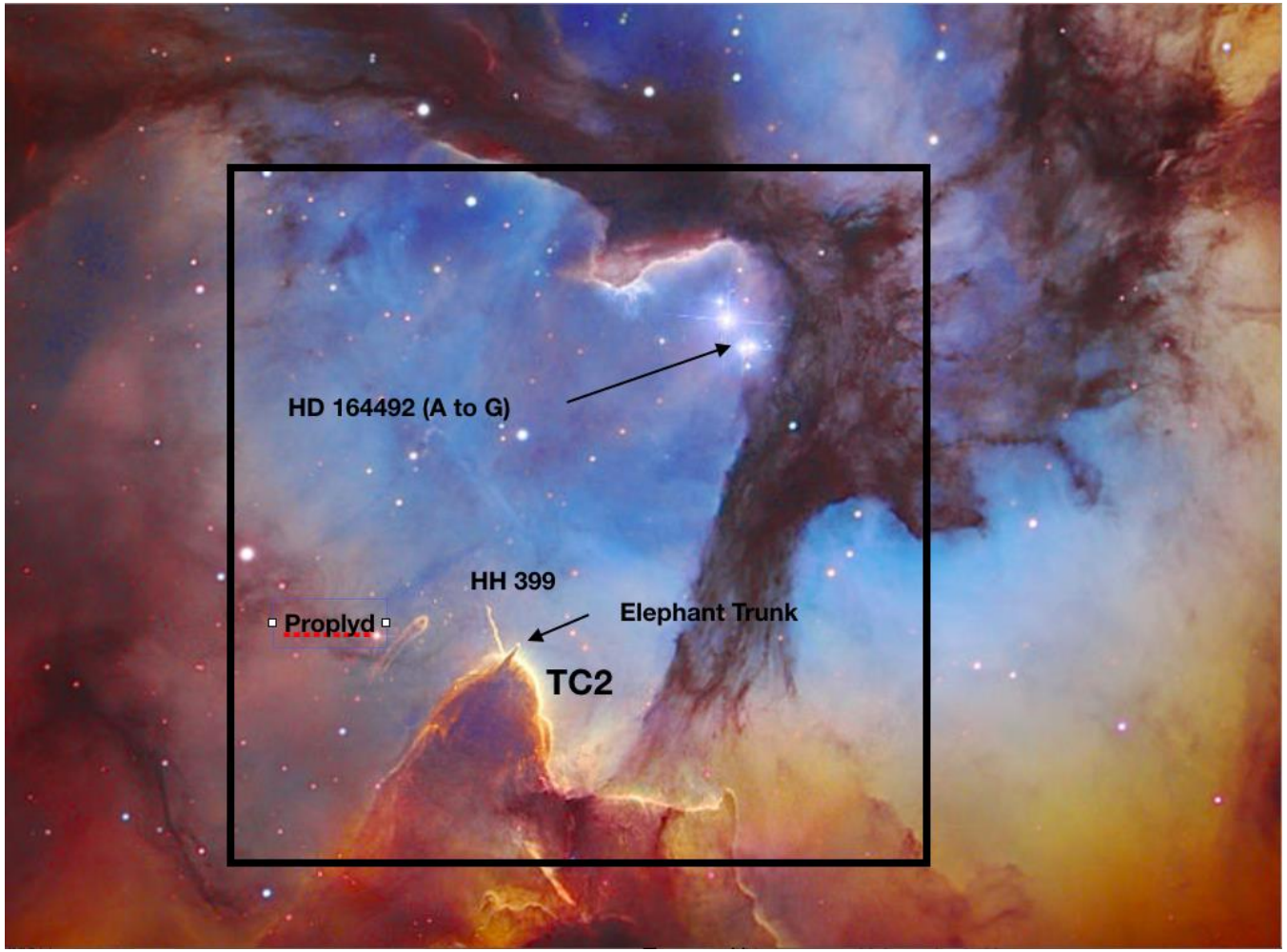

MUSE observation – Whelan et al. in prep

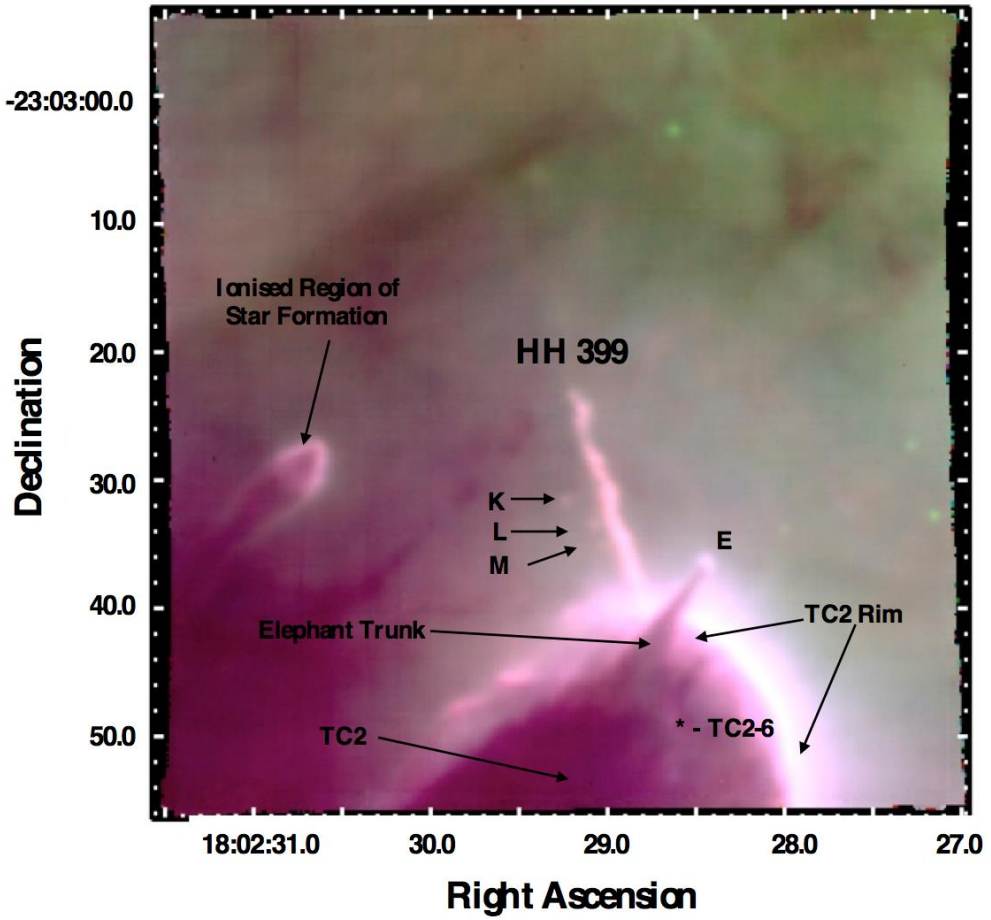

Maynooth University
National University of Ireland Maynooth

HH 399 – Spectro-Images

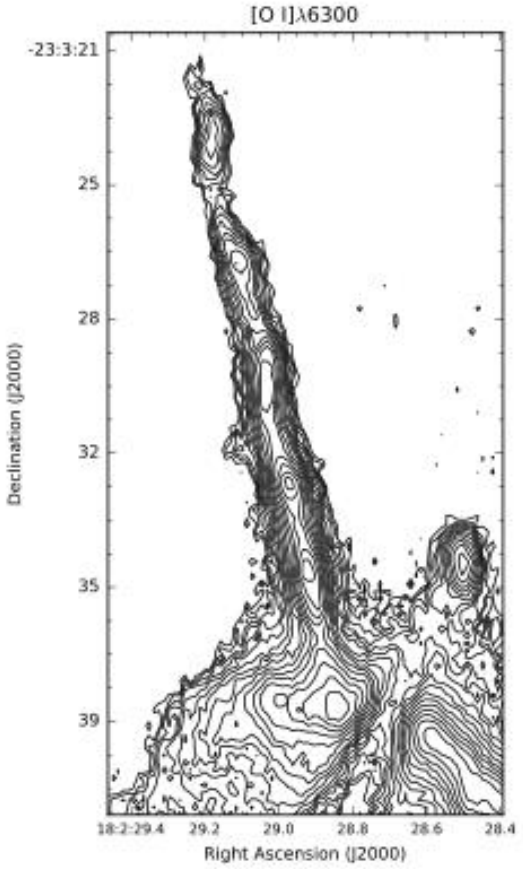

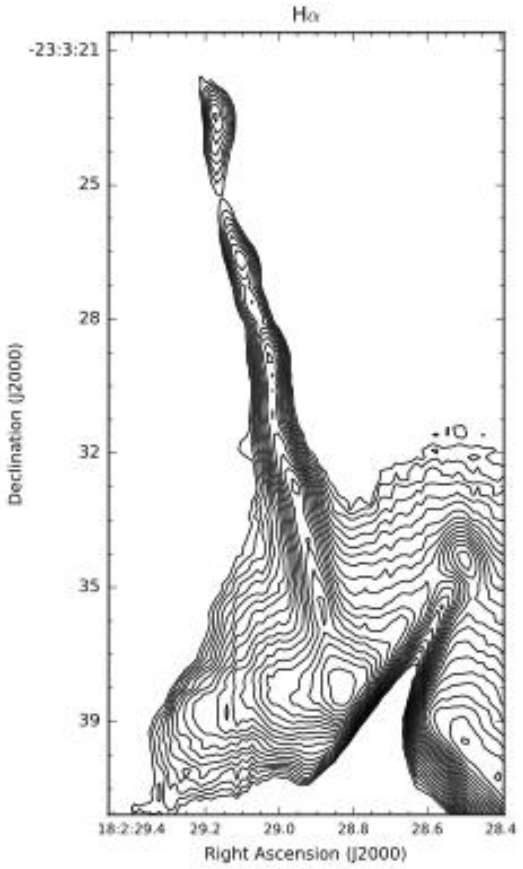

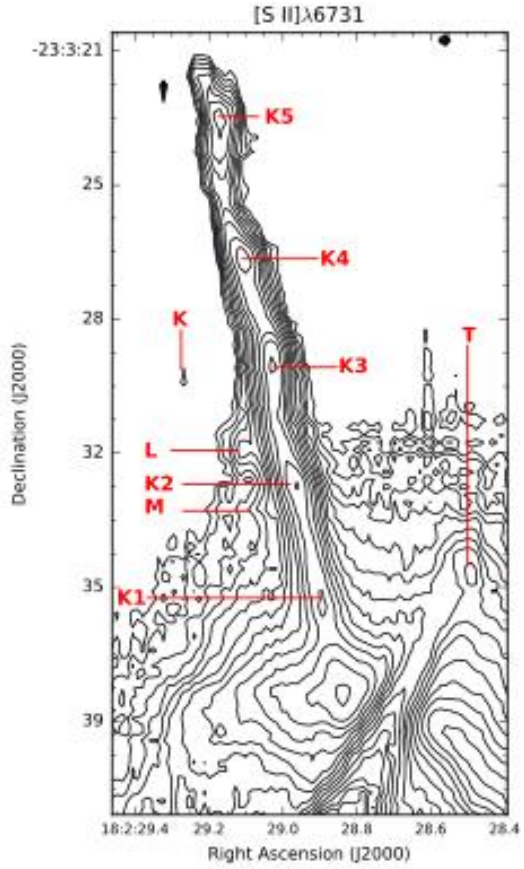

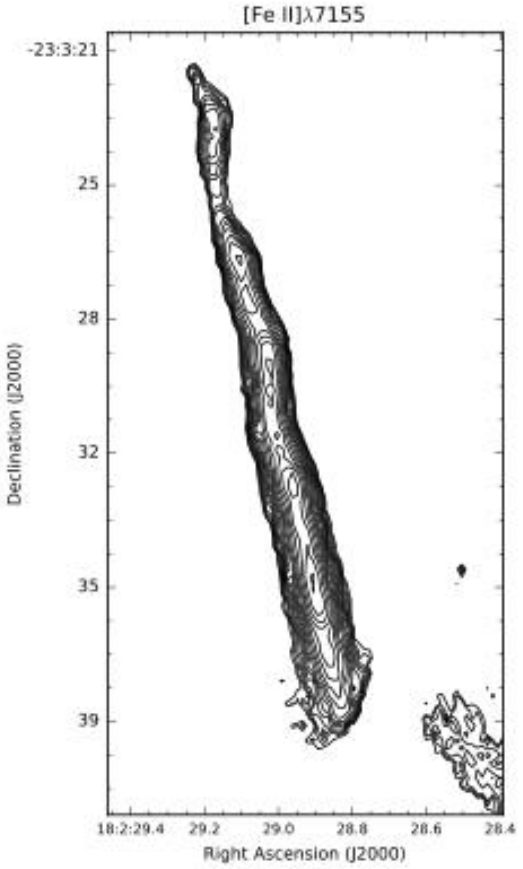

HH 399 – Spectral Analysis

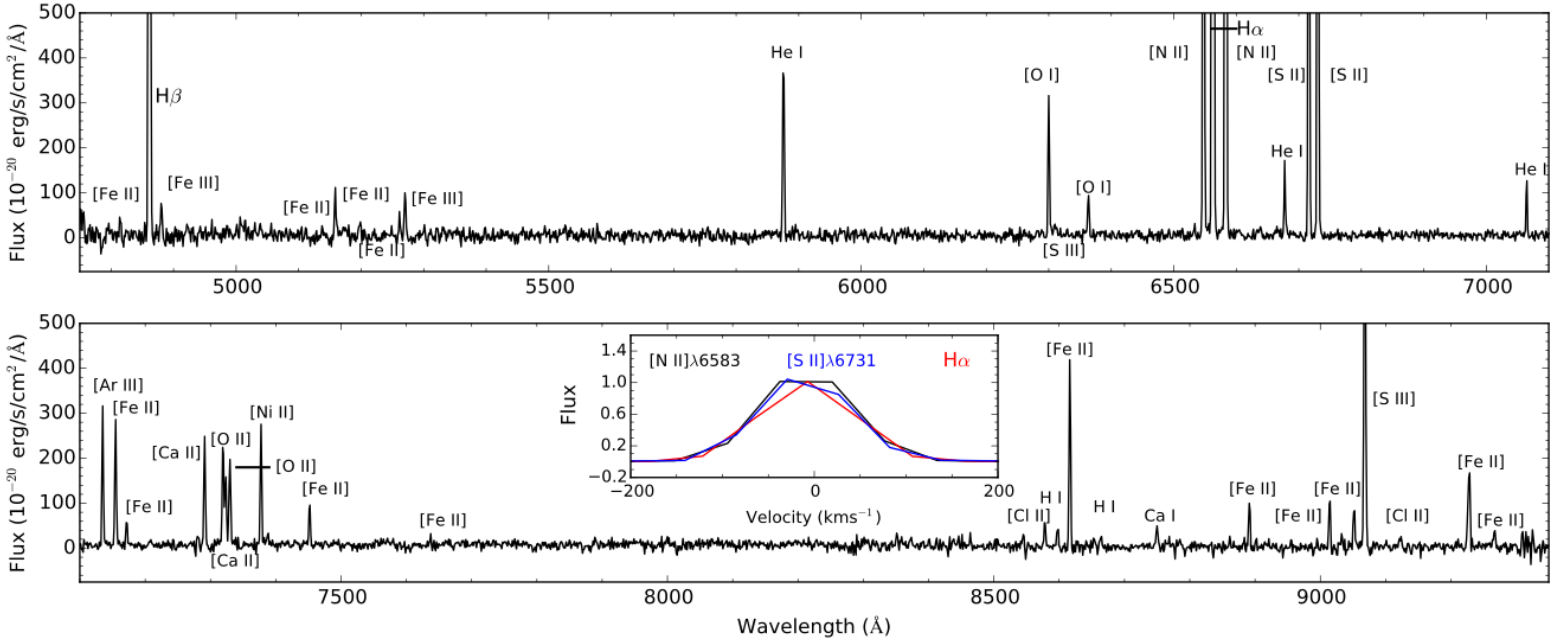

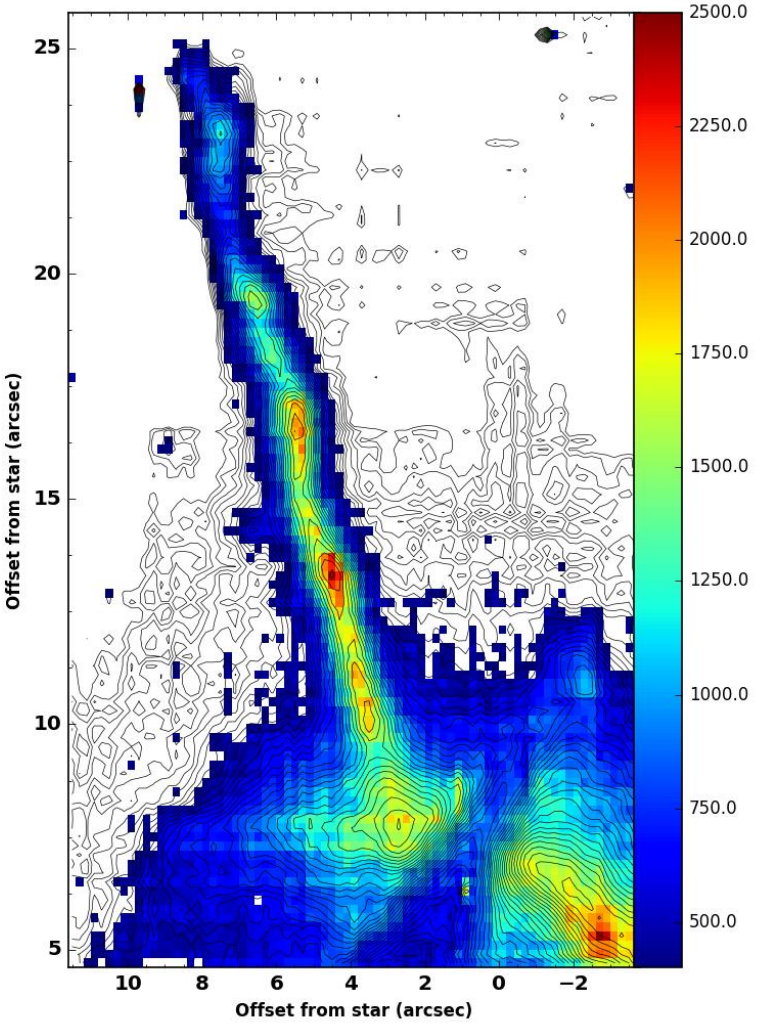

n_e in HH399 (cm^{-3})

HH 399 – Diagnostic Analysis

1. Species of both higher (Fe III, S III, Ar III) and lower excitation (Fe II, S II, Ar II) are present indicating the presence of two separate gas components. The higher density and temperature component most likely traces the central flow while the lower density and temperature component traces the outer regions of the flow.

HH 399 – Diagnostic Analysis

1. Species of both higher (Fe III, S III, Ar III) and lower excitation (Fe II, S II, Ar II) are present indicating the presence of two separate gas components. The higher density and temperature component most likely traces the central flow while the lower density and temperature component traces the outer regions of the flow.

2. Comparing emission line ratios to shock models (Hartigan+94, Ellerbroek+2014) reveal pre-shock velocities of 90-100 km/s. This is supported by the observed lack of emission in [O III] which caps the shock velocities at 100 km/s.

Ratio	Observed in HH399 K1, K2, K3, K4, K5	V_s (km s^{-1})
[O I]λ6302 / Hα	0.04, 0.04, 0.23, 0.02, 0.01	>90
[S II](λ6718+λ6733) / Hα	0.38, 0.31, 0.28, 0.27, 0.22	>90
[N II]λ6585/[O I]λ6302	13.3, 12.3, 17.6, 20.8, 41.8	~80
Hα / Hβ	3.85, 4.07, 3.97, 3.94, 4.04	40-60

Table 2. Emission lines ratios which are useful in estimating the pre-shock velocity, following table 2 of Hartigan et al. (1999) and references therein. The last two columns give the theoretical prediction for the pre-shock velocity, and the associated reference figure in Hartigan et al. (1994). Predictions are indicative, as they also depend on assumptions for pre-shock density and magnetic field.

HH 399 – Diagnostic Analysis

1. Species of both higher (Fe III, S III, Ar III) and lower excitation (Fe II, S II, Ar II) are present indicating the presence of two separate gas components. The higher density and temperature component most likely traces the central flow while the lower density and temperature component traces the outer regions of the flow.

2. Comparing emission line ratios to shock models (Hartigan+94, Ellerbroek+2014) reveal pre-shock velocities of 90-100 km/s. This is supported by the observed lack of emission in [O III] which caps the shock velocities at 100 km/s.

3. Ratios indicate that collisional processes dominate over photo-excitation in its contribution to the excitation of this irradiated jet. (However, the two knots closest to the source have notably different ratios to the two knots farther away. The requires further investigation.)

Ratio	Observed in HH399 K1, K2, K3, K4, K5	V_s (km s^{-1})
[O I]λ6302 / Hα	0.04, 0.04, 0.23, 0.02, 0.01	>90
[S II](λ6718+λ6733) / Hα	0.38, 0.31, 0.28, 0.27, 0.22	>90
[N II]λ6585/[O I]λ6302	13.3, 12.3, 17.6, 20.8, 41.8	~80
Hα / Hβ	3.85, 4.07, 3.97, 3.94, 4.04	40-60

Table 2. Emission lines ratios which are useful in estimating the pre-shock velocity, following table 2 of Hartigan et al. (1999) and references therein. The last two columns give the theoretical prediction for the pre-shock velocity, and the associated reference figure in Hartigan et al. (1994). Predictions are indicative, as they also depend on assumptions for pre-shock density and magnetic field.

Ratio	Observed in HH399 K1, K2, K3, K4, K5	Col.	Col. + Fluor.
[Ni II] Ratio			
λ7411/7377	0.08, 0.10, 0.12, ... , ...	0.05-0.07	0.34
[Fe II] Ratios			
λ4815/8892	0.26, 0.20, 0.47, 0.43, ...	0.4	0.5-4
λ4815/8617	0.08, 0.07, 0.15, 0.15, ...	~0.17	0.2-0.7
λ5334/8617	0.06, 0.05, 0.07, ... , ...	0.05-0.2	0.15-0.2
λ5334/8892	0.17, 0.13, 0.20, ... , ...	0.1-0.3	0.5-1.2
λ(7542+7155)/8617	0.66, 0.65, 0.68, 0.68, 0.68	0.6-1.0	0.3-1.0

Table 3. Emission lines ratios sensitive to fluorescence, following table 2 of Giannini et al. (2015) and references therein. The final two columns present theoretical predictions for collisional excitation alone, and collisional excitation as well as fluorescence. Observed ratios align best with predictions of collisional excitation alone. Note that the ratio (7542+7155)/8617 is effectively 7155/8617 as in these observations the [Fe II]λ7542 emission is very faint.

HH 399 – Diagnostic Analysis

1. Species of both higher (Fe III, S III, Ar III) and lower excitation (Fe II, S II, Ar II) are present indicating the presence of two separate gas components. The higher density and temperature component most likely traces the central flow while the lower density and temperature component traces the outer regions of the flow.

2. Comparing emission line ratios to shock models (Hartigan+94, Ellerbroek+2014) reveal pre-shock velocities of 90-100 km/s. This is supported by the observed lack of emission in [O III] which caps the shock velocities at 100 km/s.

3. Ratios indicate that collisional processes dominate over photo-excitation in its contribution to the excitation of this irradiated jet. (However, the two knots closest to the source have notably different ratios to the two knots farther away. The requires further investigation.)

4. Ratios of refractory to non-refractory species indicate the presence of dust in the jet, and that this dust content is lower closer to the source. This is as expected if it is assumed that the shock velocity is higher closer to the source, and so more dust is converted to gas in this region. As the jet propagates, the gas condenses into dust.

Ratio	Observed in HH399 K1, K2, K3, K4, K5	V_s (km s^{-1})
[O I]λ6302 / Hα	0.04, 0.04, 0.23, 0.02, 0.01	>90
[S II](λ6718+λ6733) / Hα	0.38, 0.31, 0.28, 0.27, 0.22	>90
[N II]λ6585/[O I]λ6302	13.3, 12.3, 17.6, 20.8, 41.8	~80
Hα / Hβ	3.85, 4.07, 3.97, 3.94, 4.04	40-60

Table 2. Emission lines ratios which are useful in estimating the pre-shock velocity, following table 2 of Hartigan et al. (1999) and references therein. The last two columns give the theoretical prediction for the pre-shock velocity, and the associated reference figure in Hartigan et al. (1994). Predictions are indicative, as they also depend on assumptions for pre-shock density and magnetic field.

Ratio	Observed in HH399 K1, K2, K3, K4, K5	Col.	Col. + Fluor.
[Ni II] Ratio			
λ7411/7377	0.08, 0.10, 0.12, ... , ...	0.05-0.07	0.34
[Fe II] Ratios			
λ4815/8892	0.26, 0.20, 0.47, 0.43, ...	0.4	0.5-4
λ4815/8617	0.08, 0.07, 0.15, 0.15, ...	~0.17	0.2-0.7
λ5334/8617	0.06, 0.05, 0.07, ... , ...	0.05-0.2	0.15-0.2
λ5334/8892	0.17, 0.13, 0.20, ... , ...	0.1-0.3	0.5-1.2
λ(7542+7155)/8617	0.66, 0.65, 0.68, 0.68, 0.68	0.6-1.0	0.3-1.0

Table 3. Emission lines ratios sensitive to fluorescence, following table 2 of Giannini et al. (2015) and references therein. The final two colur present theoretical predictions for collisional excitation alone, and collisional excitation as well as fluorescence. Observed ratios align best v predictions of collisional excitation alone. Note that the ratio (7542+7155)/8617 is effectively 7155/8617 as in these observations the [Fe II]λ7 emission is very faint.

Summary

Integral field spectroscopy allows MUSE to collect a huge amount of spectral data over an exceptionally large field of view and spectral range. This allows a large number of optical emission lines to be studied in multiple regions of a jet.

Medium spectral resolution may limit usefulness of observations for studying jet kinematics, particularly in jets with little separation of velocity components (e.g. Th28).

MUSE is primarily suited for powerful diagnostic studies, with the capacity to map physical conditions and carry out line diagnostics across a jet.

Further work to be done including on the diagnostic maps of Th28, examination of accretion luminosity, and applying MUSE tools to HD163296.